Experimental Effective Shape Control
of a Powered Transfemoral Prosthesis

Robert D. Gregg, Tommaso Lenzi, Nicholas P. Fey, Levi J. Hargrove, and Jonathon W. Sensinger

Abstract— This paper presents the design and experimental implementation of a novel feedback control strategy that regulates effective shape on a powered transfemoral prosthesis. The human effective shape is the effective geometry to which the biological leg conforms—through movement of ground reaction forces and leg joints—during the stance period of gait. Able-bodied humans regulate effective shapes to be invariant across conditions such as heel height, walking speed, and body weight, so this measure has proven to be a very useful tool for the alignment and design of passive prostheses. However, leg joints must be actively controlled to assume different effective shapes that are unique to tasks such as standing, walking, and stair climbing. Using our previous simulation studies as a starting point, we model and control the effective shape as a virtual kinematic constraint on the powered Vanderbilt prosthetic leg with a custom instrumented foot. An able-bodied subject used a by-pass adapter to walk on the controlled leg over ground and over a treadmill. These preliminary experiments demonstrate, for the first time, that effective shape (or virtual constraints in general) can be used to control a powered prosthetic leg.

I. Introduction

The *effective shape* of the human leg during locomotor tasks (called the *rollover shape* during walking) has been studied for over a decade [1] and has proven to be a very useful measure for gait analysis and prosthesis alignment [2], [3]. The effective shape is the trajectory of the center of pressure (COP)—the point on the plantar sole of the foot where the cumulative reaction force is imparted against the ground—mapped into a moving reference frame attached to the stance leg. For a rigid object, e.g., a metal wheel, the effective shape is its actual geometry. However, the effective shape of an object that includes a compliant or controllable joint—such as a human or prosthetic ankle—is variable and can be regulated, for example, within the local coordinate frame of the shank or thigh.

Able-bodied humans appear to regulate their effective shape to remain invariant across many conditions, including heel height [3], walking speed [4], and body weight [1]. This suggests the effective shape is fundamental to human locomotor control and could be useful for designing prosthetic legs that are more adaptable than conventional

prostheses, which cause discomfort and instability as these conditions vary. A passive below-knee prosthesis called the 'Shape&Roll' foot was designed to provide a natural effective shape in [5]. However, this device can only be tuned to one task at a time, whereas humans employ effective shapes unique to different tasks such as standing, walking, and stair climbing. For example, the shape curvature changes substantially between walking and stationary standing [6], and upstairs climbing requires a completely different geometry [7] with positive mechanical work.

The recent development of powered prosthetic legs (e.g., [8]–[12]) provides an opportunity to implement the effective shapes for a wide variety of tasks including those that require positive work contribution. A general model of these shapes could enable these prostheses to control different tasks with one unifying control strategy, in contrast to current task-specific approaches that depend on pre-defined reference trajectories [8], [12]. Because the effective shape characterizes the entire stance period of gait, this control approach could also improve the clinical viability of powered legs by reducing the time needed to tune control parameters compared to strategies that discretize the stance period into multiple control models [9]–[11].

For the purpose of designing this unifying control strategy, we look to recent work on autonomous bipedal robots, which can walk, run, and climb stairs using one control framework [13], [14]. This nonlinear feedback control approach produces joint torques to *virtually* enforce kinematic constraints [13]–[15], which define desired joint patterns as functions of a mechanical phase variable (e.g., the stance leg angle or hip position). In other words, a monotonic (e.g., strictly increasing) variable serves as a unique representation of the gait cycle phase, which parameterizes a nonlinear control model to create appropriate phase-specific behaviors. Because the COP is a monotonic variable [16], the effective shape can similarly be modeled as a phase-based kinematic constraint.

We recently demonstrated this principle in simulation by controlling the effective shape of an ankle prosthesis [16] and a knee-ankle prosthesis [17] during a walking task. Because the thigh-based effective shape depends on both the knee and ankle, this strategy coordinated the control of both joints to produce human-like patterns in [17]. This coordinated control approach also resulted in robustness to small perturbations. By treating the COP as a phase variable and the effective shape as a general virtual constraint for the leg joints, this novel approach has the potential to make prosthetic legs more adaptable, robust, and easily tuned than with current

Asterisk indicates corresponding author.

R.D. Gregg* is with the Departments of Mechanical Engineering and Bioengineering, University of Texas at Dallas, Richardson, TX 75080. `rgregg@utdallas.edu`

T. Lenzi, N.P. Fey, L.J. Hargrove, and J.W. Sensinger are with the Center for Bionic Medicine, Rehabilitation Institute of Chicago and the Departments of Physical Medicine & Rehabilitation and Mechanical Engineering, Northwestern University, Chicago, IL 60611.
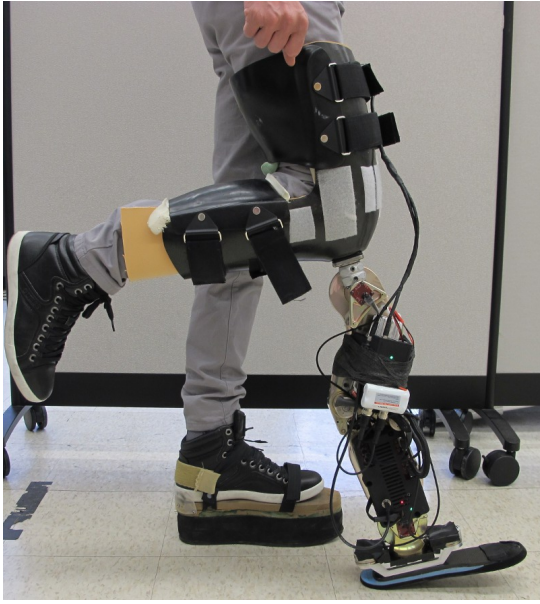
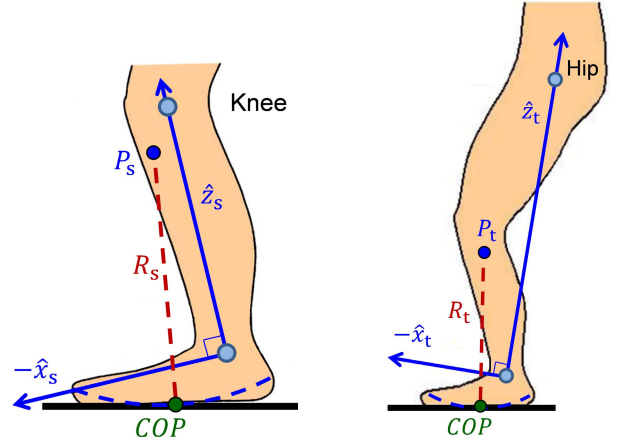Fig. 1. Image of able-bodied subject walking on the Vanderbilt prosthetic leg using a by-pass adapter.

Fig. 2. Diagrams of the ankle-foot (left) and knee-ankle-foot (center) effective shapes. The COP moves along each shape (dashed curve) in the shank-based or thigh-based coordinate frame (solid axes).

prosthetic control strategies.

In this paper we experimentally implement for the first time a control strategy using effective shape (or virtual constraints in general [13]) on a powered prosthetic leg. We designed a custom instrumented foot to provide real-time measurements of the COP to the transfemoral Vanderbilt leg from [10]. One able-bodied subject used a by-pass adapter to walk on the prosthesis (Fig. 1), both over ground and over a treadmill. The subject achieved stable walking after minimal tuning of a small set of parameters. These preliminary experiments demonstrate that regulating effective shape provides stable control that is biomimetic and that intuitively coordinates ankle-knee movement.

II. EFFECTIVE SHAPE CONTROL

The effective shape is currently only defined for the stance leg, so in this paper we focus on stance-period control (we will employ conventional impedance control during the swing period [10] for the experiments in Section III). Here we show how to model and control the effective shape.

A. Definition of Effective Shape

An effective shape characterizes how stance leg joints move as the COP travels from heel to toe. Able-bodied humans have effective shapes specific to activities such as walking [1], stationary swaying [6], and stair climbing [7], and each shape can be characterized by the curvature of the COP trajectory with respect to a reference frame attached to the stance leg. In particular, the ankle-foot (AF) effective shape is the COP trajectory mapped into a shank-based reference frame (axes $\hat{x}_s$, $\hat{z}_s$ in Fig. 2, left). This shape can be modeled by the distance between the COP and a point $P_s = (X_s, Z_s)^T$ in the shank-based reference frame:

$$||P_s - COP|| = R_s, \qquad (1)$$

where the radius of curvature R_s is approximately constant within standing and walking tasks [6].

The knee-ankle-foot (KAF) effective shape is the COP trajectory transformed into a thigh-based reference frame (axes $\hat{x}_t$, $\hat{z}_t$ in Fig. 2, center). This reference frame shares an origin with that of the AF effective shape, but the z_t-axis is attached to the thigh at the hip joint. Defining a point $P_t = (X_t, Z_t)^T$ in this reference frame, the COP moves about P_t with radius of curvature R_t. Therefore, the KAF effective shape is characterized by the distance relationship (1) with center of rotation P_t and radius R_t.

We will see that these two effective shapes provide two virtual kinematic constraints to control two joints—the ankle and knee of the prosthesis.

B. Modeling and Control

We first model the prosthetic leg as a kinematic chain with respect to a global reference frame defined at the COP during stance (Fig. 3, left). We then derive kinematic constraints for the effective shapes in the model coordinates.

The lengths of the heel, shank, and thigh segments of the leg are labeled ℓ_f, ℓ_s, and ℓ_t, respectively. The configuration of the leg is given by $q = (q_x, q_z, \phi, \theta_a, \theta_k)^T$, where q_x, q_z are the Cartesian coordinates of the heel defined with respect to the COP, ϕ is the foot orientation defined with respect to vertical, θ_a is the ankle angle, and θ_k is the knee angle. In these preliminary experiments we did not use an inertial measurement unit, so we instead defined

$$q_z = L/4 - \sqrt{(L/4)^2 - q_x^2}$$
$$\phi = 2\mathrm{sign}(q_x)\arcsin(2\sqrt{q_x^2 + q_z^2}/L),$$

for $L = \ell_s + \ell_t$, to approximate heel rise and foot rotation based on a rocker foot model from [17].

Noting that the COP coincides with the origin of the global reference frame (at $q_x = q_z = 0$ in Fig. 3, left), the effective center of rotation is given in this COP-based reference frame by the function

$$P_s^{COP}(q) = (q_x, q_z)^T + \ell_f(-\sin(\phi), \cos(\phi))^T + S(\phi + \theta_a)P_s,$$

Fig. 3. Left: kinematic model of transfemoral prosthetic leg with human subject's hip joint shown as a dashed circle. Positive/negative movement are respectively termed dorsiflexion/plantarflexion for the ankle and extension/flexion for the knee. Right: Vanderbilt leg attached to custom instrumented foot and able-bodied by-pass adapter above the knee joint. Note the mirror image is shown on the right, so as to coincide with the model on the left.

where S is the standard rotation matrix parameterized by angle $\phi + \theta_a$. Equation (1) is then given in our model coordinates by the kinematic constraint $h_s(q) = 0$ for

$$h_s(q) \quad := \quad R_s - \mathrm{norm}(P_s^{COP}(q)). \qquad (2)$$

In other words, h_s is an output of the control system corresponding to tracking error, specifically the Euclidean distance from the desired AF effective shape.

The KAF center of rotation is given in the COP reference frame by the function

$$P_t^{COP}(q) = (q_x, q_z)^T + \ell_f(-\sin(\phi), \cos(\phi))^T + S(\rho)P_t,$$

where rotation matrix S is parameterized by angle

$$\rho = \phi + \arctan\left(\frac{\ell_s \sin(\theta_a) + \ell_t \sin(\theta_a + \theta_k)}{\ell_s \cos(\theta_a) + \ell_t \cos(\theta_a + \theta_k)}\right).$$

Finally, the kinematic constraint for the KAF effective shape is given in our model coordinates by $h_t(q) = 0$, where output

$$h_t(q) \quad := \quad R_t - \mathrm{norm}(P_t^{COP}(q)). \qquad (3)$$

We wish to virtually enforce the AF and KAF constraints on the prosthetic leg, which we can achieve by producing control torques that drive outputs (2)-(3) to zero. For the experiments in this paper the prosthesis used the proportional-derivative (PD) control law

$$\begin{aligned} \tau_a &= -k_{pa}h_s(q) - k_{da}\dot{h}_s(q,\dot{q}) &(4)\\ \tau_k &= -k_{pk}h_t(q) - k_{dk}\dot{h}_t(q,\dot{q}) - k_{dka}\dot{h}_s(q,\dot{q}), \end{aligned}$$

where gains k_{pa}, k_{pk}, k_{da}, k_{dk}, and k_{dka} (held constant during the stance period) determined the desired corrective torques τ_a and τ_k at the ankle and knee, respectively. Note that the knee torque includes an ankle damping term to

Fig. 4. Top: Computer-assisted design of load cell adapter mounted on a carbon fiber prosthetic foot plate. Bottom: Assembled instrumented foot used in experiments.

facilitate knee flexion as the ankle rapidly plantarflexes during late stance.

Control law (4) is linear in the outputs $h_s(q)$, $h_t(q)$, but these outputs are nonlinear functions of the configuration q, including the COP. The x-component of the COP moves monotonically from heel to toe during steady walking, so the COP serves as the phase variable of this nonlinear controller. Control behavior will thus change continuously with the gait cycle phase, by which a single equation will control the entire stance period. This strategy was tested in simulation [16], [17] to verify stability before our experimental implementation. We discuss this implementation in the next section, beginning with the design of a custom instrumented foot that provided real-time COP measurements.

III. IMPLEMENTATION AND RESULTS

A. Instrumented Foot

We designed the instrumented prosthetic foot in Fig. 4 to measure the COP for our feedback controller. Two aluminum plates were mounted around two 6-axis load cells (model: Mini45, ATI Industrial Automation, Apex, NC) with one cell towards the heel and the other towards the toe. This configuration distributed loads encountered during walking to prevent sensor saturation and bending moments. The top plate was mounted to the bottom of the prosthetic ankle joint, and the bottom plate was mounted to a carbon fiber prosthetic foot plate; the configured leg is shown in Fig. 3, right. The assembled foot adapter (load cells and aluminum plates) added 0.79 kg to the weight of the foot plate.

The two aluminum plates of the foot adapter were mechanically coupled only through the load cells, by which we measured the loads transferred between the leg and ground for our COP calculation. We first used a free-body diagram to determine the sum of moments about the y-axis acting at the ankle joint and each of the two load cells. Each load cell measures its net moment (M_{y1} at the heel and M_{y2}

at the toe), and the ankle experiences zero net moment while the foot is flat. This provides three equations with which to solve for the x-component of the COP:

$$COP_x = \frac{-(c^2 + cd)F_{z1} + (d^2 + cd)F_{z2} + dM_{y1} + dM_{y2}}{(c + d)(F_{z1} + F_{z2}) + M_{y1} - M_{y2}},$$

where F_{z1}, F_{z2} are the vertical loads at the heel and toe, respectively, and $c = d = 0.07$ m is the horizontal length between the ankle joint and each of the load cell centers (Fig. 4, top). This equation requires only two of the six strain gauges in each load cell (this ATI model was selected primarily for compactness, weight, and load ratings), so cheaper sensors could potentially be used.

B. Vanderbilt Leg and Experimental Setup

We experimentally tested our control algorithm on the Vanderbilt leg, a powered knee-ankle prosthesis developed at Vanderbilt University (see [10] for design details). This device has encoders to measure joint angles/velocities and two actuators that provide current-level control of the knee and ankle joints. A microcontroller used sensor feedback from the leg and instrumented foot to compute the desired torques from (4), which were converted into open-loop current commands to the actuators. The prosthesis employed this controller only during the stance period, as detected by the vertical force measured by the load cells. When the load dropped below a threshold, the prosthesis entered the swing period using an impedance control approach similar to [10].

For our experiments we chose the normalized shape parameters $R_s = R_t = 0.158$ and $X_s = X_t = -0.02$ (multiplied by the user's height) according to observations[1] from able-bodied studies [4]. The constraint defined by (2) is satisfied when the COP passes through the shank-based z_s-axis, so the z_s-component of P_s is necessarily given by $Z_s = \sqrt{R_s^2 - X_s^2} - \ell_f$. Because the shank-based and thigh-based coordinate frames share an origin, the z_t-component of P_t is similarly given by $Z_t = \sqrt{R_t^2 - X_t^2} - \ell_f$. Noting that torque control law (4) depends on feedback from outputs h_s, h_t in units of m, we chose the normalized PD gains $k_{pa} = k_{pk} = 2$ N/kg, $k_{da} = k_{dk} = 0.6\sqrt{k_{pk}}$, and $k_{dka} = -0.5k_{dk}$. We arrived at these PD gains after minor adjustments of values suggested by the simulations in [17].

An able-bodied subject was fitted with a by-pass adapter (Fig. 1), allowing the subject to walk on the prosthetic leg while his/her shank trailed behind the prosthesis. The subject walked with the leg on a treadmill for 20 steps (Fig. 5) and over ground for 20 steps (Fig. 6). Here we focus on the data recorded during the stance period, when the effective shape controller was employed.

C. Results

Analysis of the kinetics and kinematics highlights the capability of the proposed controller to produce fairly biomimetic movement of the prosthetic joints. Focusing on the treadmill experiment, we see in Fig. 5 (top-left) that

[1]Note that our sign convention for X_s, X_t is opposite of that used in the Hansen studies, but our values similarly correspond to the front of the leg.

the COP moved monotonically from heel to toe, which was essential to acting as a phase variable in our control strategy.

The ankle angle trajectory in Fig. 5 (middle-right) closely matches Winter's able-bodied data [18], starting with a short period of controlled plantarflexion as the foot progressed from heel-strike to foot-flat. Subsequently as the leg rotated over the foot, the ankle started dorsiflexing until a peak of about 12 degrees was reached at about 70% of stance. The movement then reversed and the ankle started to actively plantarflex, as indicated by the torque profile in Fig. 5, middle-left (estimated from the motor current). This clearly shows that the proposed controller can provide a powered push-off at the end of stance, thus contributing actively to the energetics of walking. The ankle did not reach the physiologically appropriate peak torque because its motor saturated at 80 Nm as seen in Fig. 5 (middle-left).

The knee joint exhibited less flexion in early stance compared to natural gait (Fig. 5, bottom-right; note that knee flexion was defined in the negative direction to respect the right-hand rule). This was likely due to the subject intentionally locking the knee while loading his/her body weight on the leg, which most prosthesis users do to ensure the knee does not buckle [19]. The knee torque plot of Fig. 5 (bottom-left) does not show a subsequent extensor moment as in Winter's data, but examination of the prosthetic knee angle shows that the joint was against the hard stop (at about 4 degrees), which provided an unmeasured extensor moment. Late-stance knee flexion was close to natural and in synergy with ankle push-off, allowing the transfer of positive propulsive energy to the user. However, the knee controller appeared to produce an excessive extensor torque just before the stance-to-swing transition, resulting in a plateau of the flexion angle. This might be the result of errors in output tracking or even the torque commands due to our open-loop implementation of current control on the actuators.

The overground walking data (Fig. 6) did not show as much late knee extension as did the treadmill data, suggesting that knee extension may be exacerbated when the treadmill belt pulls the stance foot as the body unloads. A supplemental video of the overground experiment can be viewed at `http://vimeo.com/59308918`. Overall, data from the overground experiment matched that from the treadmill experiment.

IV. DISCUSSION

Our control strategy produced close-to-normal walking patterns using generic, normalized shape parameters from the literature. The use of an able-bodied subject with a prosthesis bypass was likely the main source of inconsistencies with Winter's data. A slightly prolonged mid-stance period was required to overcome the inertia added by the trailing shank, as indicated by the shallower-than-normal slope of the time-phase curve during early-to-mid stance (i.e., the COP trajectory in Fig. 5, top-left, compared to able-bodied data in [16]). Walking in this manner feels unnatural to able-bodied subjects, who typically must compensate by using hand rails. This may have altered kinetic patterns in our experiments.
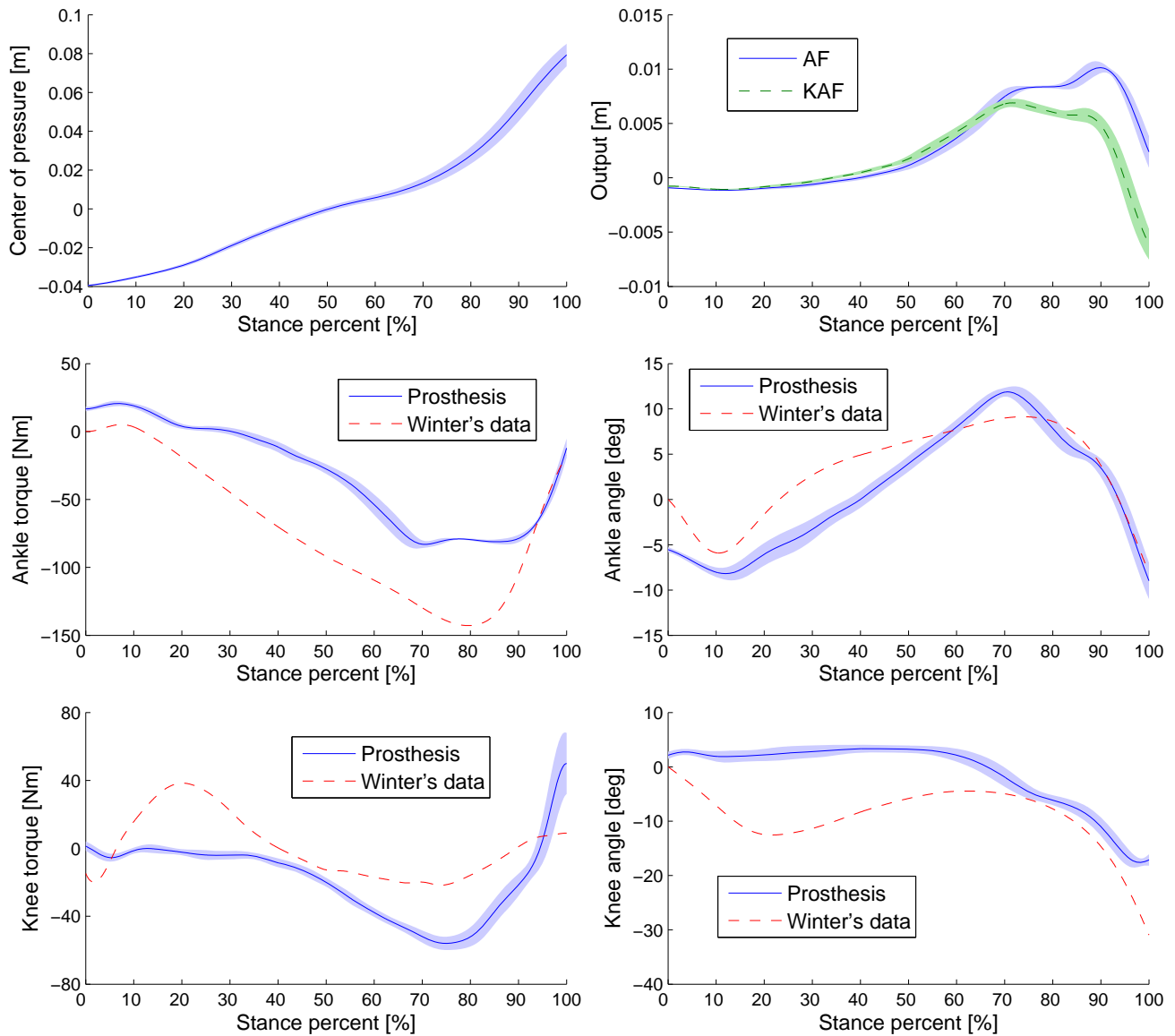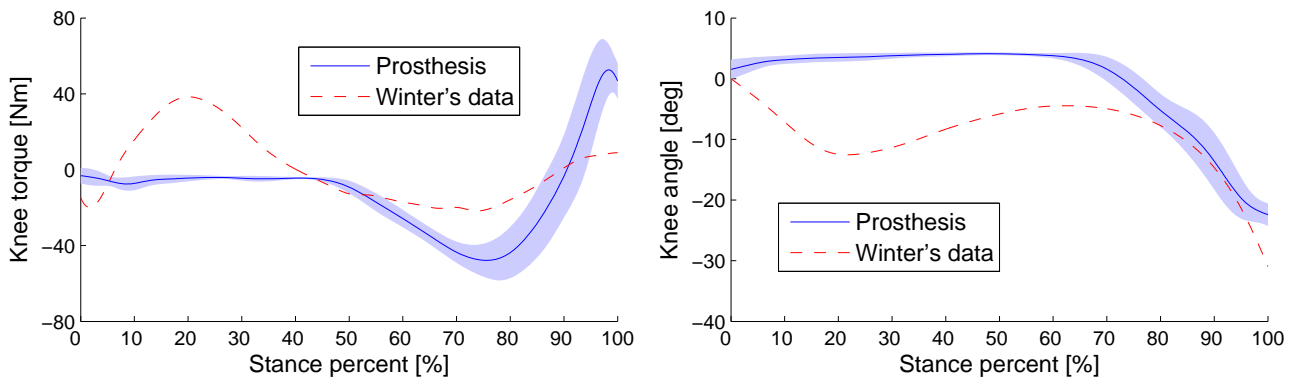
Fig. 5. Mean values (solid blue) and error bars (±1 standard deviation shown in shaded regions) of prosthesis kinematics/kinetics during treadmill walking at 2 mph for 20 gait cycles, compared with human data (dashed red) from [18]. Center of pressure (top-left), ankle/knee outputs (top-right), ankle torque and angle (middle), and knee torque and angle (bottom) over percentage of stance period. Each output (top-right) corresponds to the Euclidean distance from a desired effective shape. Note that the prosthesis torques are estimated from the open-loop motor current (and do not account for extensor moments from the knee hard stop), and the able-bodied torques from [18] are normalized by the subject's body-weight.

Fig. 6. Mean values (solid blue) and error bars (±1 standard deviation shown in shaded regions) of prosthesis knee torque (left) and angle (right) over percentage of stance period during overground walking for 20 gait cycles, compared with human data (dashed red) from [18]. Note that the prosthesis torques are estimated from the open-loop motor current, and the able-bodied torques from [18] are normalized by the subject's body-weight.

These problems will likely be avoided in future studies by recruiting transfemoral amputee subjects.

Some inconsistencies were also caused by limitations in control authority. Tracking error from the desired effective shapes (Fig. 5, top-right) grew through the step due to 1) ankle actuator saturation, 2) low-gain PD control at the joint level, and 3) open-loop current control at the motor level. We were unable to reliably increase the PD gains further because the existing control architecture limited us to a 100 Hz sampling frequency for joint-level control. In addition to implementing a faster control loop, tracking error could be greatly reduced in the future by using a more powerful ankle motor, a more exact control method such as input-output linearization [16], [17], and a closed torque-control loop at the motor level.

Despite these remaining challenges, the control framework proposed in this paper could potentially improve the clinical viability of powered transfemoral prostheses. The knee-ankle strategy used only five independent control parameters ($R_s = R_t$, $X_s = X_t$, $k_{pa} = k_{pk}$, $k_{da} = k_{dk}$, k_{dka}) for the entire stance period, whereas other control approaches have many more parameters during stance (e.g., 18 for sequential impedance control [10], 14 for one joint's muscle model [11], or an entire look-up table for tracking human data [12]). The effective radii R_s, R_t and rotational centers X_s, X_t are defined by simple fractions of the user's height [4], offering a straight-forward tuning procedure for clinicians. The rotational centers determine the amount of flexion in the ankle and knee joints, respectively, so these characteristics can be systematically adjusted to the user's preference.

Coordination and synchrony between leg joints in human locomotion (e.g., through biarticular muscles) are important to energetic efficiency [20] and robustness [17], but coordinated control is uncommon in current multi-joint prostheses. Our strategy coordinated knee control with the ankle joint to enforce the KAF shape, which explicitly depends on the ankle angle in (3). Knee and ankle patterns were also synchronized by their dependence on the same phase variable, the COP. The stability of this control approach was formally verified in the simulations of [16], [17], and our initial experiments appear to confirm this finding. In particular, we observed convergence to a periodic orbit—known as a limit cycle—in the phase portrait of Fig. 7, suggesting that the controller helped stabilize a steady-state gait pattern for the subject.

We did not explicitly design a push-off phase into the control strategy, but enforcing the effective shape provided a natural period of power generation as the COP approached the toe. A positive feedback loop arises when COP movement causes a plantarflexive ankle torque, which in turns causes the COP to move further forward. During early stance this positive loop is counteracted by a negative loop involving the moment arm from shear forces. This biomimetic behavior, resembling that of more complex muscle reflex models [11], might prevent compensatory work at the hip [21] and allow lower-limb amputees to expend normal levels of energy when walking.
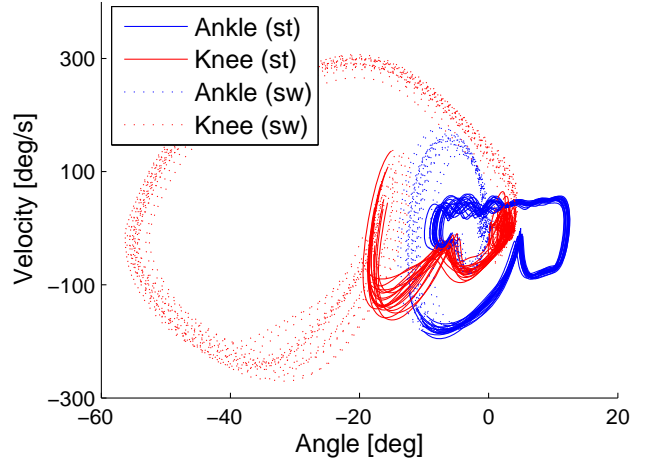

Fig. 7. Phase portrait (angular positions vs. velocities) of 20 gait cycles (stance period shown as solid line and swing as dashed line) from treadmill experiment. The ankle and knee trajectories appear to converge to a periodic orbit—known as a limit cycle—as the subject's gait approached steady state. Note that most of the variability occurs during the swing period, when the prosthesis employed a conventional sequential impedance controller.
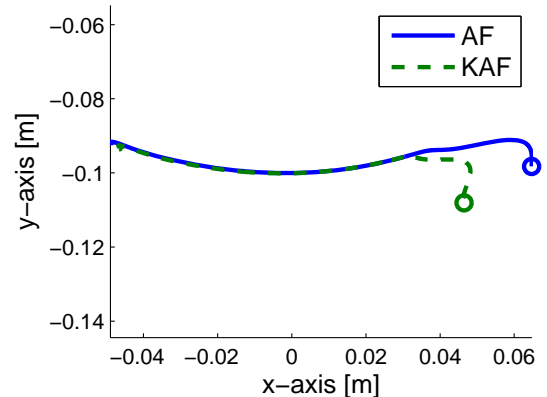

Fig. 8. Mean rollover shapes (i.e., COP trajectory in a shank- or thigh-based reference frame) from treadmill experiment. End of stance is indicated by a circle. Note that a 'hook' occurs during double support, which resembles able-bodied rollover shapes [4].

The push-off period ends during double leg support, when the stance leg lifts off the ground to become the swing leg of the next step. The curvature of the effective shape is not constant during the double-support period in able-bodied walking [1], but for simplicity we continued to control the constant-curvature constraints (2)-(3) as the prosthesis entered double support with the intact leg. This may have contributed to the large knee extensor torque observed during double support. We see in Fig. 8 that the PD controller provided compliance in the rollover shape during double support (matching able-bodied shapes), so inexact tracking may have been beneficial in this case. The loading threshold that triggered the swing-period controller also influenced leg behavior at the end of this period. The appropriate prosthesis behavior during double support requires further investigation.

V. CONCLUSION

This paper presented the first ever experiments using effective shape (or any form of virtual constraint [13]) for the control of a powered prosthetic leg. These preliminary experiments demonstrate that this control strategy can stably produce biomimetic and coordinated ankle-knee movement on a real prosthetic leg, confirming the simulation results of [16], [17]. These findings will be tested in future experiments with transfemoral amputee subjects. The proposed control strategy could also be evaluated across various conditions such as heel height, walking speed, and body weight to verify invariance as observed with the biological leg [1].

This paper only concerned the stance period of gait, but an ideal prosthetic control system would also employ phase-based virtual constraints during the swing period. However, the COP is not defined for the swing leg. Effective shapes could possibly be modeled between swing leg joints and a different phase variable, which is left to future work.

The proposed control approach can also regulate the effective shapes for different tasks including inclined walking and stair climbing. For this purpose the controller can employ a more general model of effective shape—allowing non-constant curvature in (2) and (3)—from [17]. Effective shape control could then be integrated with a neural interface (e.g., using electromyography from residual muscles [22]) to allow the user to subconsciously adapt the effective shapes when anticipating a task change.

For more demanding tasks like running, a more exact control law may be needed to prevent output tracking error. An input-output linearizing control law is derived in [16], [17] that can theoretically regulate effective shapes with zero tracking error. This work will require accurate system identification of the intrinsic dynamics of the prosthetic leg.

The role of the COP in the effective shape begs questions about the possible use of this phase variable in human locomotor control. Phase-based virtual constraints could also be applied to powered orthoses [23], [24] and exoskeletons [25]. With further development the proposed control concepts have the potential to improve mobility and quality of life for individuals after amputation, stroke, or spinal cord injury.

REFERENCES

[1] A. Hansen and D. Childress, "Investigations of roll-over shape: Implications for design, alignment, and evaluation of ankle-foot prostheses and orthoses," *Disability & Rehabilitation*, vol. 32, no. 26, pp. 2201–2209, 2010.

[2] A. Hansen, D. Childress, and E. Knox, "Prosthetic foot roll-over shapes with implications for alignment of trans-tibial prostheses," *Prosth. Orth. Int.*, vol. 24, no. 3, pp. 205–215, 2000.

[3] A. Hansen and D. Childress, "Effects of shoe heel height on biologic rollover characteristics during walking," *J. Rehab. Res. & Development*, vol. 41, no. 4, pp. 547–554, 2004.

[4] A. Hansen, D. Childress, and E. Knox, "Roll-over shapes of human locomotor systems: Effects of walking speed," *Clinical Biomechanics*, vol. 19, no. 4, pp. 407–414, 2004.

[5] M. Sam, D. Childress, A. Hansen, M. Meier, S. Lambla, E. Grahn, and J. Rolock, "The 'Shape&Roll' prosthetic foot: I. Design and development of appropriate technology for low-income countries," *Medicine, Conflict & Survival*, vol. 20, no. 4, pp. 294–306, 2004.

[6] A. Hansen and C. Wang, "Effective rocker shapes used by able-bodied persons for walking and fore-aft swaying: Implications for design of ankle-foot prostheses," *Gait & Posture*, vol. 32, no. 2, pp. 181–184, 2010.

[7] E. Sinitski, A. Hansen, and J. Wilken, "Biomechanics of the ankle-foot system during stair ambulation: Implications for design of advanced ankle-foot prostheses," *Journal of Biomechanics*, vol. 45, pp. 588–594, 2012.

[8] Össur, "POWER KNEE," 2012. [Online]. Available: http://www.ossur.com/powerknee/.

[9] F. Sup, A. Bohara, and M. Goldfarb, "Design and control of a powered transfemoral prosthesis," *Int. J. Robotics. Res.*, vol. 27, no. 2, pp. 263–273, 2008.

[10] F. Sup, H. Varol, and M. Goldfarb, "Upslope walking with a powered knee and ankle prosthesis: Initial results with an amputee subject," *IEEE Trans. Neural Systems & Rehab. Engineering*, vol. 19, no. 1, pp. 71–78, 2011.

[11] M. Eilenberg, H. Geyer, and H. Herr, "Control of a powered ankle–foot prosthesis based on a neuromuscular model," *IEEE Trans. Neural Systems & Rehab. Engineering*, vol. 18, no. 2, pp. 164–173, 2010.

[12] M. A. Holgate, T. G. Sugar, and A. W. Bohler, "A novel control algorithm for wearable robotics using phase plane invariants," in *IEEE Int. Conf. Robotics & Automation*, 2009, pp. 3845–3850.

[13] E. R. Westervelt, J. W. Grizzle, C. Chevallereau, J. H. Choi, and B. Morris, *Feedback Control of Dynamic Bipedal Robot Locomotion*. New York, NY: CRC Press, 2007.

[14] K. Sreenath, H. W. Park, I. Poulakakis, and J. W. Grizzle, "A compliant hybrid zero dynamics controller for stable, efficient and fast bipedal walking on MABEL," *Int. J. Robotics Res.*, vol. 30, no. 9, pp. 1170–1193, 2011.

[15] E. R. Westervelt, J. W. Grizzle, and D. E. Koditschek, "Hybrid zero dynamics of planar biped walkers," *IEEE Trans. Automatic Control*, vol. 48, no. 1, pp. 42–56, 2003.

[16] R. D. Gregg and J. W. Sensinger, "Towards biomimetic virtual constraint control of a powered prosthetic leg," *IEEE Trans. Control Sys. Tech.*, 2013, in press.

[17] ——, "Biomimetic virtual constraint control of a transfemoral powered prosthetic leg," in *Amer. Control Conf.*, Washington, DC, 2013.

[18] D. A. Winter, *Biomechanics and Motor Control of Human Movement*. New York, NY: Wiley, 2009.

[19] K. Kaufman, J. Levine, R. Brey, B. Iverson, S. McCrady, D. Padgett, and M. Joyner, "Gait and balance of transfemoral amputees using passive mechanical and microprocessor-controlled prosthetic knees," *Gait & Posture*, vol. 26, no. 4, pp. 489–493, 2007.

[20] A. Pedotti, "A study of motor coordination and neuromuscular activities in human locomotion," *Biological Cybernetics*, vol. 26, no. 1, pp. 53–62, 1977.

[21] J. Johansson, D. Sherrill, P. Riley, P. Bonato, and H. Herr, "A clinical comparison of variable-damping and mechanically passive prosthetic knee devices," *Amer. J. Phys. Med. & Rehab.*, vol. 84, no. 8, pp. 563–575, 2005.

[22] L. Hargrove, A. Simon, R. Lipschutz, S. Finucane, and T. Kuiken, "Real-time myoelectric control of knee and ankle motions for transfemoral amputees," *J. Amer. Med. Assoc.*, vol. 305, no. 15, pp. 1542–1544, 2011.

[23] R. D. Gregg, T. W. Bretl, and M. W. Spong, "A control theoretic approach to robot-assisted locomotor therapy," in *IEEE Conf. Decision and Control*, Atlanta, GA, 2010, pp. 1679–1686.

[24] K. Shorter, J. Xia, E. Hsiao-Wecksler, W. Durfee, and G. Kogler, "Technologies for powered ankle-foot orthotic systems: Possibilities and challenges," *IEEE/ASME Trans. Mechatronics*, vol. 18, no. 1, pp. 337–347, 2013.

[25] A. Dollar and H. Herr, "Lower extremity exoskeletons and active orthoses: Challenges and state-of-the-art," *IEEE Trans. Robotics*, vol. 24, no. 1, pp. 144–158, 2008.